Journal of Visualization, Vol. 2, Nos. 3/4 (2000) 213-221

A PIV Study of a Supersonic Impinging Jet

Elavarasan, R.*[1], Venkatakrishnan, L.*[1], Krothapalli, A.*[2] and Lourenco, L.*[3]

*[1] Research Associate, Department of Mechanical Engineering,Florida A&M University and Florida State University, Tallahassee, Florida 32310, USA.
*[2] Don Fuqua Eminent Scholar and Professor,Department of Mechanical Engineering, Florida A&M University and Florida State University, Tallahassee, Florida 32310, USA.
*[3] Professor, Department of Mechanical Engineering, Florida A&M University and Florida State University, Tallahassee, Florida 32310, USA.

Received 4 March 1999.
Revised 17 September 1999.

***Abstract*:** The characteristics of supersonic impinging jets are investigated using Particle Image Velocimetry (PIV). The purpose of the experiments is to understand the jet induced forces on STOVL aircraft while hovering close to the ground. For this purpose, a large diameter circular plate was attached at the nozzle exit. The oscillations of the impinging jet generated due to a feedback loop are captured in the PIV images. The instantaneous velocity field measurements are used to describe flow characteristics of the impinging jet. The important flow features such as oscillating shock waves, slipstream shear layers and large scale structures are captured clearly by the PIV. The presence of large scale structures in the impinging jet induced high entrainment velocity in the near hydrodynamic field, which resulted in lift plate suction pressures. A passive control device is used to interfere with the acoustic waves travelling in the ambient medium to suppress the feedback loop. As a consequence, the large scale vortical structures disappeared completely leading to a corresponding reduction in the entrainment.

***Keywords*:** supersonic impinging jets, PIV, large scale structures, convection velocity, feedback control.

1. Introduction

High speed jet impingement can occur in many aerospace applications such as in Short Take-Off and Vertical Landing (STOVL) aircraft. The characteristics of supersonic jet impingement induced effects especially during the landing and take-off are crucial in such applications. STOVL aircraft experience a suck down force known as "lift loss" while hovering close to the ground. The lift loss is caused by the jet induced low surface pressure on the airframes and results in a force opposite to lift. The magnitude of the lift loss increases when the distance between the aircraft and ground decreases. In addition to the lift loss, significant ground erosion occurs while the aircraft is in the vertical landing mode. The jet induced oscillation is also a source of intense noise with levels reaching up to 180 dB.

In addition to the known sources of sound from free supersonic jets, such as mixing noise and shock associated noise (Tam, 1995), additional discreet tones are produced by the impingement of the jet on a ground plate. The discrete tones are known to be generated by a feedback mechanism. Many investigations have been carried out to confirm the generation of impingement tone by feedback mechanism (Neuwerth, 1974; Powell, 1988; Tam and Ahuja, 1990; Henderson and Powell, 1993). The reflected acoustic waves from the ground upon reaching the nozzle exit, excite the initial shear layer and induce instability. The instability waves grow as they propagate downstream and manifest themselves as large structures. These structures in turn generate pressure fluctuations, which intensifies the acoustic waves further. More information about the feedback mechanism can be

found in Neuwerth (1973), Ho and Noisseir (1981), Powell (1988), Tam and Ahuja (1990), Henderson and Powell (1993) and Krothapalli et al. (1999).

Limited information is available at present in order to characterize supersonic impinging jet induced effects. In the present study, experiments are carried out to provide some understanding of the physics of the flow and the role of large-scale structures in noise generation. The Particle Image Velocimetry technique proved to be the ideal choice for such studies as it provides both qualitative and quantitative information of the whole flow field. The impinging jet configuration chosen for the present experiment resembles that used by number of earlier investigators (Marsh, 1961; Neuwerth, 1974; Powell, 1988; Tam and Ahuja, 1990; Messersmith, 1995; Kuo and Dowling, 1996). The only difference in the present experimental arrangement is the lift plate attached to the nozzle, which simulates the airframe of the STOVL aircraft.

2. Experimental Arrangement

The experiments were conducted in STOVL experimental facility at Fluid Mechanics Research Laboratory at Florida State University. The details of the facility were given in Wardwell et al. (1993). Two different nozzles were used in the present investigation. A converging axisymmetric (conical) nozzle was used to simulate an under expanded, choked jet flow and a shock free nearly ideally expanded jet was obtained using an axisymmetric converging-diverging (CD) nozzle. The throat diameter is 2.54 cm for both nozzles and the CD nozzle had a 3^0 diverging angle at the exit. The exit diameters (d) for conical and CD nozzles are 2.54 and 2.74 cm respectively. The nozzle upstream of the throat was designed using a third order polynomial with a contraction ratio of approximately 5. The designed exit Mach number is 1.5 for the CD nozzle.

In order to simulate the STOVL aircraft in hover, the nozzle was flush mounted with a circular plate of diameter D (25.4 cm), as shown in Fig. 1. The diameter of the lift plate was 25.4 cm (approximately 10-nozzle exit diameter). A large Plexiglas ground plate of size 117×91×2.54 cm was mounted on a hydraulic lift, which can be moved relative to the nozzle. Varying the distance between the ground plate and the nozzle simulates the effect of hovering in and out of the ground. A high-pressure blow down compressed air facility provides the air supply to the jet, which is driven by a high displacement reciprocating air compressor. The maximum capacity of the storage tank is 10^3 m^3. The facility can be run at an exit Mach number 1.5 for about 40 minutes continuously.

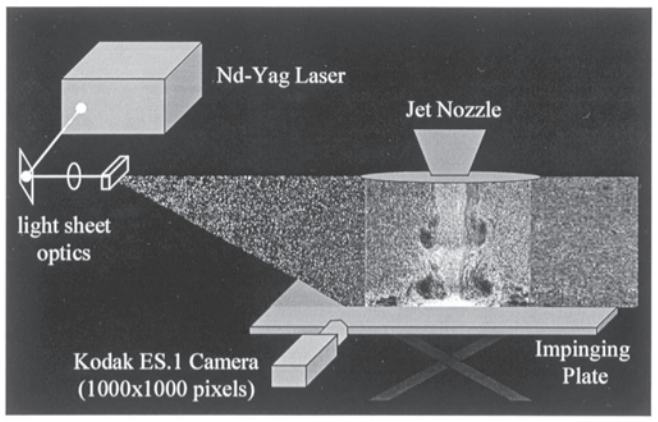

Fig. 1. The schematic of the experimental setup.

The main controlling parameters in the experiment were: the Nozzle Pressure Ratio (NPR = stagnation pressure/ambient pressure); the ground plate height h with respect to the nozzle exit. The NPR was varied from 2.5 to 5. The ground plate height, h was varied from $4d$ to $60d$ (free jet). The typical Reynolds number at the nozzle exit was about 7×10^5 for a stagnation temperature of 20˚C. The co-ordinates x and r correspond to axial and radial directions of the jet and u and v are the respective velocity components.

For PIV measurements, a double pulsed digitally sequenced Nd:YAG laser (Spectra-Physics, 400 mJ) was used. A light sheet of one mm thickness was created by suitable combination of spherical and cylindrical lenses. The images were recorded by a cross correlation CCD camera (Kodak ES1.0) whose axis was perpendicular to the flow axis. The resolution of the camera is 1k × 1k and is operated in double pulsed mode. In this mode of operation, with proper synchronization with laser pulses, the camera can acquire double images at a rate of 15

image pairs per second. Although it was possible to cover a larger area, the present measurements were restricted to 150 × 150 mm square section in the region close to the nozzle exit. The time between pulses was optimized at 2 μs. The double pulsed images were acquired through an Imaging Technologies ICPCI board, which resides on a single slot of the PCI bus of a personal computer. The images were analyzed using a rectangular grid of 125 × 125 (maximum) interrogation cells. The size of each interrogation cell is 8 × 8 pixels (1 pixel=0.18 mm). For each case described in the present paper, 80 instantaneous double exposed images were collected. The time it takes to compute a vector field depends on the computer hardware and it ranges from 350 mesh points/sec to 1,400 mesh points/sec on a 300 MHz Pentium-II PC.

An in-house developed cross correlation algorithm based on Fourier Transformation is then used to extract the velocity information from the double exposed images. The algorithm uses a novel mesh free approach, which resolve the bias errors inherent with the standard PIV processing technique as it does not suffer from the interrogation region boundaries. This also provides data with high spatial resolution and computes each particle image pair and associated position with second order accuracy which is maintained by the least squares approach for error minimization (Lourenco, 1998).

The selection of the seeding particles for PIV measurements depends on many parameters such as large seeding density, ability to withstand the high temperature and pressure fluctuations, size, cost and safety. The success of the measurements depends on the proper choice of the seeding particles. In the present experiment, the jet was seeded with oil droplets (~1 μm) generated by a Wright Nebulizer, which delivered the particles to the main jet. The flow rate of the seeding particles was controlled in such a way that there were enough particles in the jet. The ambient air was seeded with smoke particles (~2 μm) produced by a Rosco fog generator. It was noticed that the entrainment of 2 μm ambient seeding particles into the main jet did not affect the flow dynamics significantly.

Ross (1993) using a similar PIV apparatus carried out a careful study of the particle behavior in shock containing supersonic flow. The particle relaxation length varies significantly with the shock strength and the particle diameter. The relaxation length was about 7 mm for 1 μm particle diameter with an associated shock strength parameter ($\Delta p/p$) of 1.2. In the present experiment, the compression in the flow results in much smaller values of the shock strength parameter and as a result, the relaxation lengths are expected to be much smaller. In the absence of shock cells, the velocity of the particles was found to be in close agreement (±2%) with the calculated exit velocity using isentropic relations. A more careful investigation needs to be carried out to assess the particle behavior in the regions of large velocity gradients such as those found in the large scale vortical structures. However, it is expected that the effects of shocks and the large scale vortical structures do not significantly alter the conclusions reached in this investigation.

3. Results and Discussion

All the PIV measurements are confined to the central plane of the jet. Figures 2a-2d show the typical double exposure particle images of free jets (with ground plane height at h/d=60) and the impinging jet (h/d=4) for NPR=3.7. The main difference between the free and impinging jet is the presence of discernable large scale vortical structures in the impinging jets. These large scale structures seemed to be almost symmetrical and upon impinging on the ground plane they move laterally along the plate as a wall jet. The size of the large scale structures is almost comparable to the width of the jet. The under expanded free jet shown in Fig. 2c clearly shows the compression and expansion regions indicated by the variation in particle concentration. The effect of the impingement appears to alter the shock cell structure as shown in the under expanded case in Fig. 2d. Close to the impingement region, a standoff shock as indicated by the arrow is observed. It was also noticed that the location of standoff shock varies in concert with the shedding frequency of the large scale structures. Additional normal shocks appear upstream of the impingement region. For example, a normal shock is located at x/d = 2.47 in Fig. 2d.

Figures 3a-3d show the instantaneous velocity fields corresponding to the particle images in Figs. 2a-2d. The processing of the PIV images was carried out with a 120×80 mm (x, r) Cartesian grid. The length of the vectors corresponds to the magnitude of the velocity. The color contours represent the magnitude of the out of plane component of vorticity. The velocity and vorticity data are plotted in the laboratory reference frame. At each operating condition, 80 such instantaneous velocity fields were obtained.

The free shear layers along the edges are clearly marked and location and size of the large scale coherent structures are identified from the concentrated contour levels. The velocity variations within the shock cell structure are captured with fidelity. Except in the immediate regions following the shocks, the magnitude of the velocity is estimated to be within ±1%.

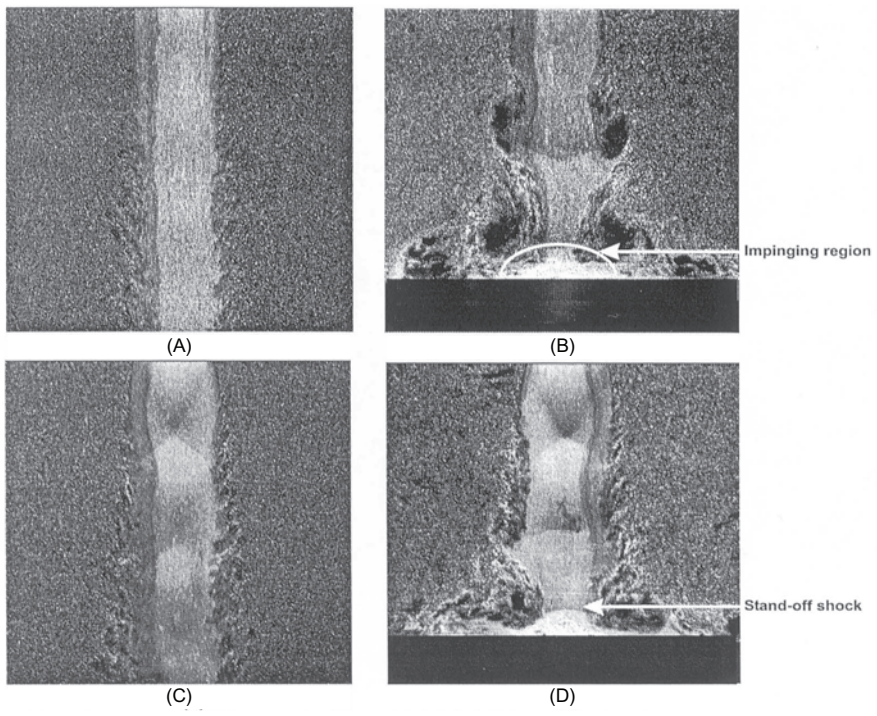

Fig. 2. Instantaneous PIV images at NPR=3.7. a) Free jet, M_d=1.5; b) Impinging jet, *h*/*d* =4; c) Free jet, M_d=1.0; d) Impinging jet, *h*/*d* =4.

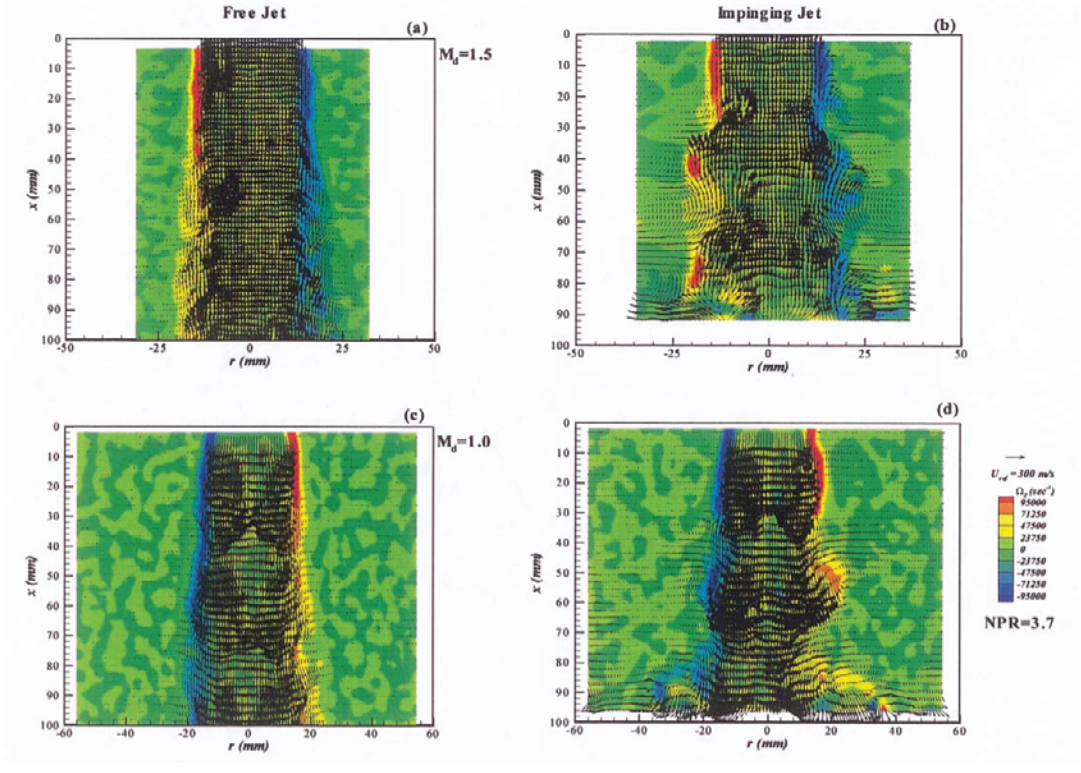

Fig. 3. Instantaneous velocity and vorticity field corresponding to the images in Fig. 2.

Figure 4 shows an enlarged view (at NPR=3.7, M_d=1.0) of a typical vortical structure in the shear layer of an impinging jet. The vortical structure is identified by the contours of the concentrated vorticity. Associated with the structure is a large entrainment field as shown in the figure. As will be disused later, this entrainment velocity field is mostly responsible for the low surface pressures on the lift plate. Once a structure is identified, its convection velocity can be easily obtained from the following procedure. As shown in Fig. 4, an imaginary line is drawn across a well-defined vortical structure. By averaging the measured velocity values at the boundaries of each contour level, it is possible to estimate the velocity with which the center of the vortical structure is convecting along the flow direction. In each instantaneous velocity field all prominent vortical structures are identified and the velocity gradient across them are measured. This procedure is repeated for all 80 frames. The convection velocity of the structure at a given downstream location is then obtained by averaging several of the instantaneous measurements.

For a free jet, the value of the convection velocity was measured to be about $0.6U_j$ (U_j=mean jet exit velocity), which is consistent with previous observations obtained using phase locked flow visualization pictures. However, in the case of an impinging jet, the convection velocity varies as a function of the ground plane height and NPR as shown in Figs. 5a, b. In order to get an overall picture about the behavior of large scale structures at different operating condition, the convection velocity is normalized with respect to the jet exit velocity corresponding to an ideally expanded jet. For an ideally expanded jet, the convection velocity varies almost linearly with *h/d* as shown in Fig. 5a. When the ground plane height is increased beyond *h/d*=15, the convection velocity of the structures reaches a free jet value of $0.6U_j$. In the presence of shock cell structure, a non-monotonic

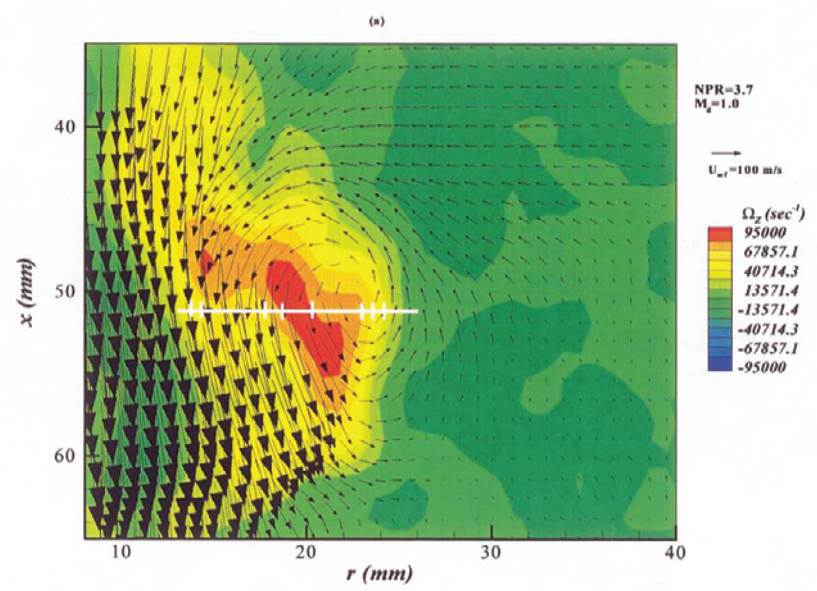

Fig. 4. Details of a large scale vortical structure.

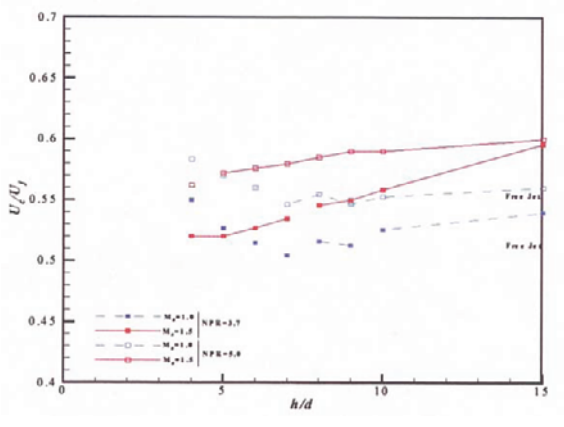

Fig. 5. Variation of convection velocities of large scale structures with *h/d*.

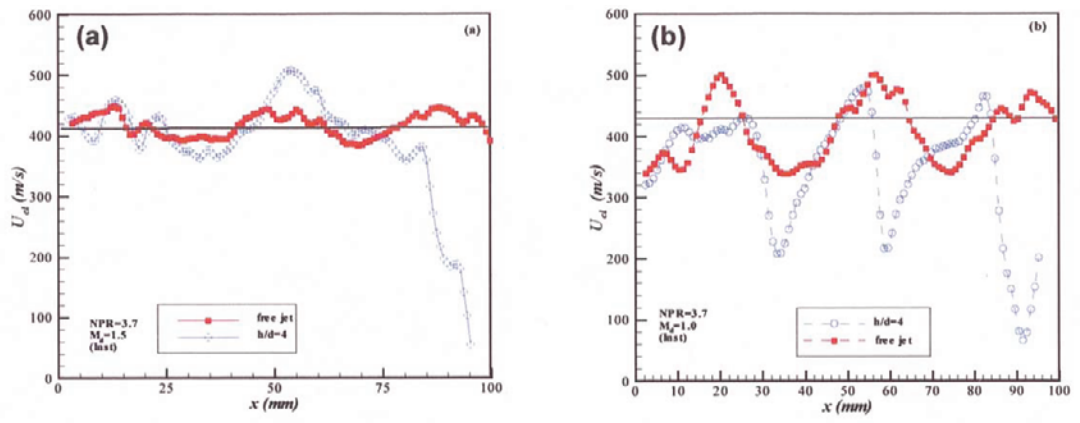

Fig. 6. Instantaneous centerline velocity variation.

behavior in the variation of the convection velocity is observed. This may be the result of non-uniform axial velocity variation in the jet as shown in Fig. 6. The reduction in the magnitude of the convection velocity due to the presence of shock cells is clearly evident from the data.

To observe the significant changes due to the impingement process, the instantaneous centerline velocity variation corresponding to the conditions in Figs. 2a-2d are plotted in Fig. 6. In the case of a nearly ideally expanded free jet, the magnitude of the centerline velocity varies about ±20 m/sec (Fig. 6a) from the nozzle exit velocity. For an impinging jet, further downstream, the flow gradually decelerates while approaching the ground plane. In contrast, the axial centerline velocity variation of the underexpanded jet shown in Fig. 6b displays an almost periodic variation of the velocity magnitude due to the presence of the shock-cell structure. The presence of the ground plane appears to affect the entire jet column along with a more drastic deceleration downstream of x~84 mm (x/d~3.3), indicating the presence of much stronger shock than the ideally expanded case. Indeed, the flow visualization clearly indicates the presence of a normal shock, commonly referred to as a standoff shock. Ideally, the velocity gradient across a normal shock will be extremely high. However, due to particle lag inherent in PIV measurements, the velocity gradient across strong shock will be somewhat smeared as evident in Fig. 6b. The location of the standoff shock varies with time and the resulting flow in the impingement region is quite unsteady.

From the examination of all the instantaneous velocity fields, it is observed that critical changes in the jet flow field of an ideally expanded jet primarily occur in the vicinity of the jet impingement region. This region extended as much as one jet diameter upstream of the ground plane. For an underexpanded jet, it appears that the entire jet column is affected by the presence of the plate and as a result, the shock cell structure is significantly modified by the impingement.

The large scale eddies, while convecting downstream, induced velocities of large magnitude in the near hydrodynamic field, which results in high entrainment along the shear layer of the jet. The magnitude of the surface pressure on the lift plate is closely linked to the jet entrainment velocities, especially when the jet is confined by two solid boundaries (lift and ground plates). These velocities can be easily obtained from PIV data. Typical instantaneous velocity variations with downstream distance at a radial location of 1.5d measured at various instances are shown in Fig. 7. The magnitude of the near field instantaneous entrainment velocity, q (= $(u^2+v^2)^{1/2}$) for a free jet is about 8 m/sec, while for the impinging jet, it is as high as 50 m/sec, as indicated by the peaks in the velocity plot shown in Fig. 7. Such large velocities in the near hydrodynamic field correspond to the presence of large vortical structures (Fig. 2b). These high entrainment velocities will result in suction pressures on the bottom surface of the lift plate resulting in a downward force (lift loss). The entrainment field is quite unsteady as can be seen from the figure. The locations of the peaks in this plot are associated with the positions of the large scale structures in the shear layer. The large velocities seen in the region x>75 mm corresponds to radial wall jet. The thickness of the radial wall jet changes with time as suggested by the location of the peak velocity magnitude close to the ground plane (x>75 mm).

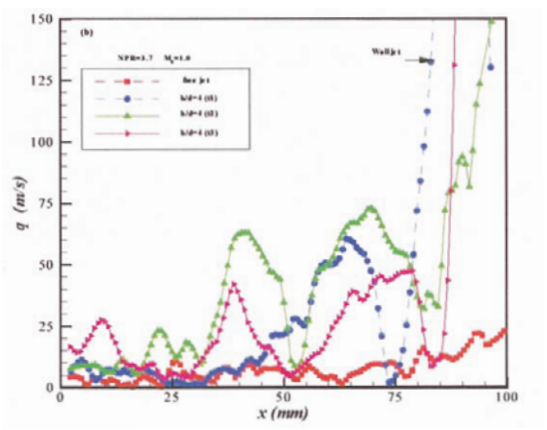

Fig. 7. Instantaneous entrainment velocity variation at different instances.

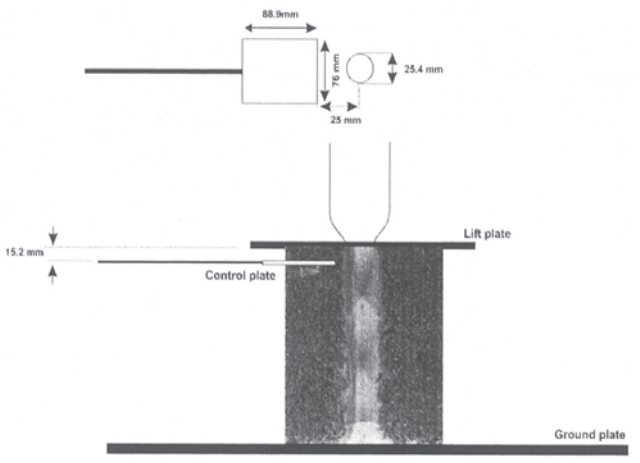

Fig. 8. Schematic of the feedback suppression experiment.

The PIV results discussed above suggest that the downward force on the lift plate is the result of entrainment flow of the large structures within the impinging jet. These large structures are believed to be created by a feedback mechanism that exists between the impinging plate and the nozzle exit. The relation between the feedback mechanism, self sustaining oscillation and sound generation in supersonic jet are described in detail by Krothapalli et al. (1999). Based on this observation, a simple passive control technique was used to weaken the feedback loop there by reducing the oscillations of the jet. The control technique uses a rectangular plate to stop the upstream propagating acoustic waves in the ambient medium from reaching the nozzle exit. A rectangular control plate (88.9mm × 76mm × 2.5mm) made of aluminum was fixed close to the nozzle exit (25 mm from the lift plate) as shown in Fig. 8.

Figure 9 shows a typical picture of an impinging jet with and without the control plate. The large structures, which are responsible for large entrainment flow, are clearly seen in Fig. 9a corresponding to the uncontrolled case. In the presence of the control plate (Fig. 9b), the shear layers do not exhibit any large scale vortical structures. From a number of such instantaneous pictures it was also observed that the standoff shock was quite steady.

The corresponding velocity fields, shown in Fig. 10, support the above observation. A stronger evidence of the lack of large scale structures and their associated entrainment velocity in the near hydrodynamic field is clearly seen in Fig. 11. Here the entrained velocity for the uncontrolled case has a large magnitude and the peaks corresponds to the location of the large scale structures.

When the control plate is present, the entrained velocity is much smaller in magnitude and is comparable to

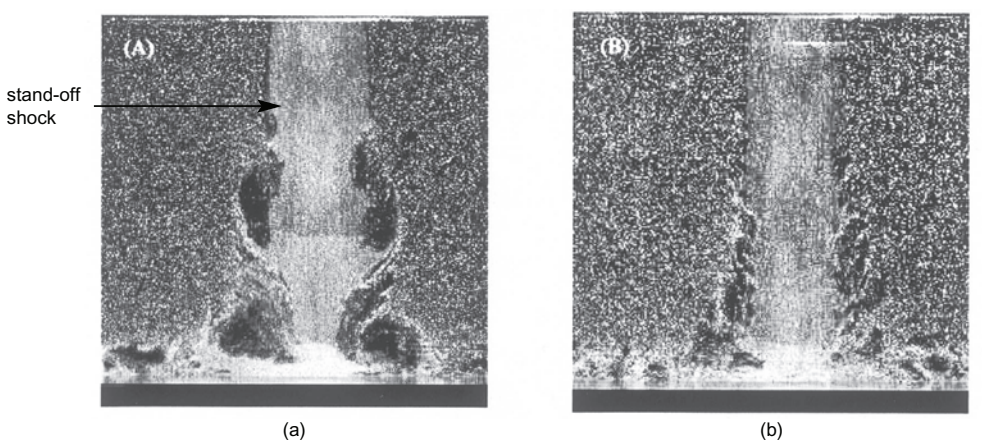

Fig. 9. Instantaneous PIV images for *h*/*d*=4 and NPR=3.7. a) Uncontrolled case; b)Controlled case.

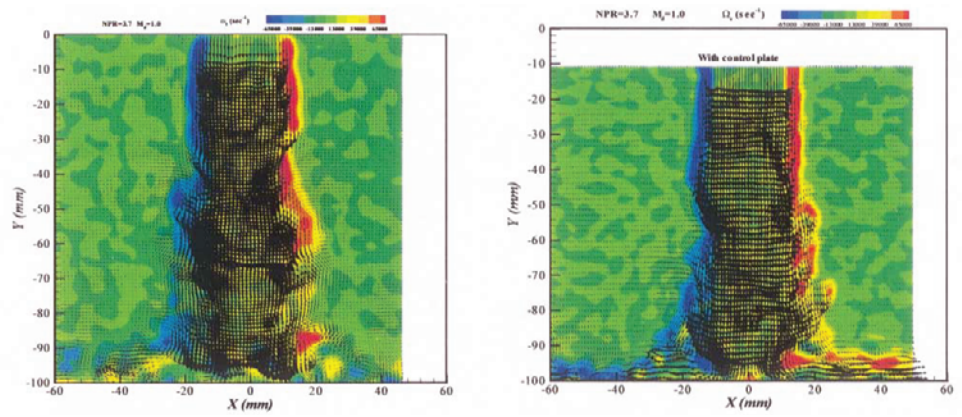

Fig. 10. Instantaneous velocity fields corresponding to the images in Fig. 9.

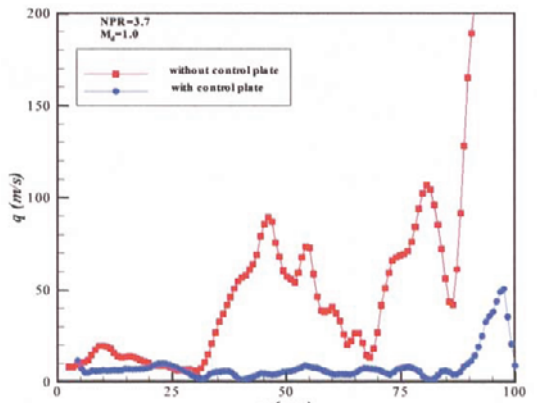

Fig. 11. Instantaneous entrainment velocity corresponding to the images in Fig. 9.

that of a free jet. In addition, the velocities in the wall jet are also significantly reduced. These results indicate that a simple passive technique to eliminate the feedback loop can be effective in eliminating the production of large scale coherent vortical structures that are primarily responsible for the lift loss.

4. Conclusion

The PIV technique has been successfully used to study highly unsteady supersonic impinging jets. Understanding the flow behavior of impinging supersonic jets is important in predicting the mean and unsteady loads on the airframe from which the jets are issuing. The self sustained oscillatory behavior of the impinging supersonic jets generates large scale coherent vortical structures in the flow. These structures play a major role in generating relatively large entrainment velocities in the near hydrodynamic field. The increased entrainment field explains the increase in the suction force on the lift plate, which results in a lift loss. When the distance between the ground plane and the nozzle exit decreases, both flow visualization and the whole field velocity data, clearly showed that the large scale structures grow stronger. The increased strength of the large scale structures resulted in a corresponding increase in the entrainment velocity in the vicinity of the nozzle exit. From a practical perspective, knowledge of the entrainment flow is essential towards an understanding of the lift loss mechanism.

The self sustaining oscillation frequencies of the jet are predicted using a feedback mechanism. Models describing this mechanism require knowledge of the convection velocity of large scale vortices in the shear layer. Using the vorticity as a tracer quantity, the convection velocities of the large scale structures in the impinging jets were measured accurately. It was found that when the jet is operating in close proximity to the ground plane, the convection velocity of the structures is smaller than that of free jets.

A significant reduction in lift loss can be accomplished by eliminating the self sustained oscillations of the jet. For example, the feedback mechanism responsible for the jet oscillations could be suppressed and stopped by placing a small plate normal to the centerline of the jet in the outside ambient flow region.

Acknowledgments

The authors acknowledge and thank the continued support of NASA Ames Research Center.

References

Henderson, B. and Powell, A., "Experiments Concerning Tones Produced by an Axisymmetric Choked Jet Impinging on Flat Plates," J. of Sound and Vibration, 168-2 (1993), 307-326.

Ho, C. M. and Nosseir, N.S., "Dynamics of an Impinging Jet. Part 1. The Feedback Phenomenon," J. Fluid Mech., 105 (1981), 119-142.

Krothapalli, A., Rajakuperan, E., Alvi, F. and Lourenco, L., "Flow field and noise characteristics of a supersonic impinging jet," J. Fluid Mech. 392 (1999), 155-187.

Kuo, C. Y. and Dowling, A. P., "Oscillations of a Moderately Underexpanded Choked Jet Impinging upon a Flat Plate," J. Fluid Mech., 315 (1996), 267-291.

Lourenco, L. M., "A 3-D High resolution PIV," in preparation (2000).

Messersmith, N. L. "Aeroacoustics of Supersonic and Impinging Jets," AIAA 95-0509, Aerospace Sciences Meeting, January (1995).

Neuwerth, G. "Acoustic Feedback of a Subsonic and Supersonic Free Jet which Impinges on an Obstacle," NASA TT F-15719 (1974).

Powell, A., "The Sound-Producing Oscillations of Round Underexpanded Jets Impinging on Normal Plates," J. Acoust. Soc. Am., 83-2 (1988), 515-533.

Ross, C. B. "Calibration of particle image velocimetry in a shock-containing supersonic flow," MS thesis, Department of Mechanical Engineering, Florida State University (1993).

Tam, C. K. W. and Ahuja, K. K, "Theoretical Model of Discrete Tone Generation by Impinging Jets," J. Fluid Mech., 214 (1990), 67-87.

Tam, C. K. W. "Supersonic Jet Noise," Annual Review of Fluid Mechanics, 27 (1995), 17-43.

Wardwell, D. A., Hange, C., Kuhn, R.E., and Stewart, V. R., "Jet-Induced Ground Effects on a Parametric Flat-Plate Model in Hover," NASA TM 104001 (1993).

Author Profile

R. Elavarasan: He received his Ph.D. in Fluid Mechanics at Indian Institute of Science, Bangalore, India in 1993. From 1994 to 1997 he worked as post doctoral fellow at University of Newcastle, Australia. He came to USA and was working at Kansas State University before joining to the Mechanical Engineering Department of Florida State University in 1998. His research interests are optical diagnostic techniques for fluid mechanics measurements, cloud dynamics, impinging jets, turbulent boundary layer control, mixing, biomedical fluid mechanics and combustion.

L. Venkatakrishnan: He obtained his Ph.D. in Fluid Mechanics at Indian Institute of Science, Bangalore, India in 1997, and is currently a post doctoral fellow at the Fluid Mechanics Research Laboratory, Florida State University. His research interests include turbulent jets and plumes, cloud physics, impinging jets, turbulent mixing and aeroacoustics.

Anjaneyulu Krothapalli: He is the Don Fuqua Eminent Scholar, Professor and Chairman of Mechanical Engineering at Florida A&M and Florida State Universities, Tallahassee. Professor Krothapalli obtained his Ph.D. in Aeronautical and Astronautical Engineering from Stanford University in 1979. He has been on the faculties of Aerospace Engineering at the University of Oklahoma (1979-1980) and the Department of Aeronautics and Astronautics at Stanford University (1981-1983). His research interests include: aeroacoustics, aero-dynamics, jets, wakes and optical diagnostics.

Luis Lourenco: He is a Professor of Mechanical Engineering jointly at Florida A&M and Florida State Universities in Tallahassee. Professor Lourenco received his D. Sc. from the University of Brussels, Belgium in 1982. His research interests include: biomedical and biofluids engineering, experimental methods, optical diagnostics, two-phase flows and heat transfer.